

REPORT DOCUMENTATION PAGE				Form Approved OMB No. 0704-0188	
Public reporting burden for this collection of information is estimated to average 1 hour per response, including the time for reviewing instructions, searching existing data sources, gathering and maintaining the data needed, and completing and reviewing this collection of information. Send comments regarding this burden estimate or any other aspect of this collection of information, including suggestions for reducing this burden to Department of Defense, Washington Headquarters Services, Directorate for Information Operations and Reports (0704-0188), 1215 Jefferson Davis Highway, Suite 1204, Arlington, VA 22202-4302. Respondents should be aware that notwithstanding any other provision of law, no person shall be subject to any penalty for failing to comply with a collection of information if it does not display a currently valid OMB control number. <b>PLEASE DO NOT RETURN YOUR FORM TO THE ABOVE ADDRESS.</b>					
1. REPORT DATE (DD-MM-YYYY) 29-06-2010		2. REPORT TYPE Final Technical Report		3. DATES COVERED (From - To) Jul.1,2006 - Dec.31,2009	
4. TITLE AND SUBTITLE Self-Organized Quantum Dots for High-Performance Multi-Spectral Infrared Photodetectors				5a. CONTRACT NUMBER FA9550-06-1-0481	
				5b. GRANT NUMBER AFOSR FA9550-06-1-0481	
				5c. PROGRAM ELEMENT NUMBER	
6. AUTHOR(S) Anupam Madhukar and Joe C. Campbell				5d. PROJECT NUMBER	
				5e. TASK NUMBER	
				5f. WORK UNIT NUMBER	
7. PERFORMING ORGANIZATION NAME(S) AND ADDRESS(ES)  University of Southern California      University of Virginia Department of Chemical Engineering and      Dept. Electrical & Comp. Eng. Materials Sciences 3651 Watt Way, VHE 502      351 McCormick Road Los Angeles, CA 90089-0241      Charlottesville, VA 22904-4743				8. PERFORMING ORGANIZATION REPORT NUMBER	
9. SPONSORING / MONITORING AGENCY NAME(S) AND ADDRESS(ES) AFOSR/NE 875 N. Randolph St. Room 3112 Arlington VA 22203				10. SPONSOR/MONITOR'S ACRONYM(S)	
				11. SPONSOR/MONITOR'S REPORT NUMBER(S) AFRL-OSR-VA-TR-2012-0586	
12. DISTRIBUTION / AVAILABILITY STATEMENT Approved for public release; distribution unlimited.					
13. SUPPLEMENTARY NOTES The view, opinion, and/or findings in this report are those of the author(s) and should not be constructed as an official Department of the Air Force position, policy, or decision, unless so designated by other documentation.					
14. ABSTRACT This AFRL Nanotechnology Initiative program focused on uncovering and overcoming the fundamental limiting factors in realizing high performance self-assembled quantum dot (SAQD) based infrared photodetectors (QDIPs) in the mid-infrared (MIR,3-5µm) and/or long wavelength infrared (LWIR, 8-12µm) regime. This Final Technical Report summarizes the major accomplishments made in this program. The highlights include: (1) successful growth of extended defect-free multiple quantum dot (MQD) structures maintaining high intra- and layer-to-layer uniformity of the SAQDs, (2) analysis of electron occupancy in SAQDs and the potential profile in QDIP structures to guide doping optimization, (3) identification, characterization, and reduction of deep level traps existing in the MBE (molecular beam epitaxy)grown GaAs spacer layers by a factor of 20 and their impact on QDIP electrical characteristics, and (4) the design and implementation of resonant cavity-enhanced QDIP structures for QDIP performance enhancement by a factor of over ten.					
15. SUBJECT TERMS Self-Assembled Quantum Dots, Quantum Dot Infrared Photodetectors, Deep Level Traps, Resonant Cavity, Mid Infrared, Long-Wavelength Infrared, Photodetector, Molecular Beam Epitaxy, Gallium arsenide, Indium arsenide, lattice strain.					
16. SECURITY CLASSIFICATION OF:			17. LIMITATION OF ABSTRACT  UU	18. NUMBER OF PAGES  12	19a. NAME OF RESPONSIBLE PERSON Anupam Madhukar
a. REPORT Unclassified	b. ABSTRACT Unclassified	c. THIS PAGE Unclassified			19b. TELEPHONE NUMBER (include area code) 213-740-4325

# **Final Technical Report**

Grant No. FA9550-06-1-0481

## **Self-Organized Quantum Dots for High-Performance Multi-Spectral Infrared Photodetectors**

Period: July 1, 2006 - December 31, 2009

**Program Managers:** Donald Silversmith (AFOSR)

### **PI:**

Anupam Madhukar  
University of Southern California  
Los Angeles, CA 90089-0241  
Tel. (213) 740-4325  
e-mail: madhukar@usc.edu

### **Co-PI:**

Joe C. Campbell  
University of Virginia  
Charlottesville, VA 22904-4743  
Tel. (434) 243-2068  
e-mail: jccuva@virginia.edu

### **Research Collaborators:**

Gail J. Brown (AFRL / WPAFB)  
Krishnamurthy Mahlingam (AFRL / WPAFB)  
Zhaoqiang Fang (Write State University)

**Abstract:** This AFRL Nanotechnology Initiative sponsored program was focused on addressing fundamental limiting factors in realizing high performance quantum dot infrared photodetectors (QDIPs) in the mid-infrared (MIR, 3 – 5  $\mu\text{m}$ ) and long wavelength infrared (LWIR, 8 – 12  $\mu\text{m}$ ) regimes. This Final Technical Report summarizes the major accomplishments under this program. The highlights include: (1) Successful growth of extended defect-free multiple quantum dot (MQD) structures without compromising the intra- and layer-to-layer uniformity of the self-assembled quantum dots (SAQDs); (2) Analysis of the electron occupancy of the SAQDs and self-consistent potential profile in the QDIP structures to extract guiding criteria for doping optimization; (3) Identification, characterization, and reduction of deep level traps in the QDIPs and their influence on QDIP electrical characteristics; and (4) Design and implementation of resonant cavity-enhanced QDIP structures for QDIP performance enhancement by over an order of magnitude.

## Table of Contents

<b>I. Objectives .....</b>	<b>3</b>
<b>II. Major Accomplishments .....</b>	<b>3</b>
<b>II.1 Formation of extended defect-free MQD structures with unimodal           size and shape distribution at desired photoresponse wavelengths .....</b>	<b>3</b>
<b>II.2 Self-consistent charge distribution and electric potential profile           in QDIP structures and its impact on QDIP characteristics .....</b>	<b>5</b>
<b>II.3 Study of deep levels present in SAQD structure and their effect on           electrical characteristics of SAQD devices .....</b>	<b>6</b>
<b>II.4 Design and implementation of resonant cavity-enhanced QDIP .....</b>	<b>9</b>
<b>III. List of Personnel .....</b>	<b>10</b>
<b>IV. List of Publications .....</b>	<b>11</b>
<b>V. Conference presentations .....</b>	<b>12</b>

## **Final Technical Report**

**AFOSR Grant No. FA9550-06-1-0481: “Self-Organized Quantum Dots for High-Performance Multi-Spectral Infrared Photodetectors”** (Jul. 1, 2006- Dec. 31, 2009)

**Program Managers:** Donald Silversmith (AFOSR); Kitt Reinhardt (AFOSR)

**P.I.** Anupam Madhukar (USC); **Co-PI:** Joe C. Campbell (UVa);

**Collaborators:** Gail J. Brown (AFRL / WPAFB); Krishnamurthy Mahalingam (AFRL / WPAFB); Zhaoqiang Fang (Wright State University)

### **I. Objective**

This research program sponsored by the AFRL Nanotechnology Initiative was undertaken to elucidate and overcome the fundamental difficulties and limitations to realization of high-performance self-assembled quantum dot (SAQD) based infrared photodetectors (QDIPs) for the mid-infrared (MIR, 3 – 5  $\mu\text{m}$ ) and long-wavelength infrared (LWIR, 8 – 12  $\mu\text{m}$ ) regimes. Considerable theoretical and experimental studies have been devoted to QDIPs for more than a decade, motivated by the advantages of QDs such as sensitivity to normal incident photons and by theoretical expectations that the use of QDs for IR detector can surpass the performance of existing quantum well IR photodetectors (QWIPs). However, the performance of QDIPs has not reached the expectations. This, as the studies undertaken in this program revealed, is largely due to the fundamental difficulties in realizing high quality multiple SAQD (MQD) structures with sufficiently low density of deep level generating defects in appropriately designed device structures. Specifically, the issues lay in (a) growth of extended defect-free MQD structures with large numbers of uniform SAQD layers that exhibit photoresponse in the desired MIR and/or LWIR regimes, (b) identification of the self-consistent electron density distribution and potential profile in QDIP structures, and their manipulation by an appropriate doping profile to maximize photocurrent (PC) while dark current (DC) is minimized, and (c) low external quantum efficiency of QDIPs (typically < 10 %) owing to the short optical path length arising from the difficulty to realize defect-free MQD structures as stated in (a) above. For this sponsored program, we have demonstrated solutions to overcome the fundamental issues noted under (a), (b) and (c). In particular, this study revealed new findings regarding deep traps and their densities accompanying traditional SAQD growth approaches versus growth procedures and conditions employed in our approach that reduces the deep trap density by a factor of ~20. Additionally, we demonstrate an enhancement in the QDIP performance by over an order of magnitude by the placement of the SAQDs at locations in a cavity indicated to be optimal through design simulations of resonant cavity QDIPs. The following provides summary of the highlights achieved in this program. Details can be found in the publications listed in Sec. IV.

### **II. Major Accomplishments**

#### **II. 1 Growth of extended defect-free MQD structures with unimodal size and shape distribution of SAQDs at desired photoresponse wavelengths**

**Publication:** Tetsuya Asano, Anupam Madhukar, Krishnamurthy Mahalingam, and Gail J. Brown, “Dark current and band profiles in low defect density thick multilayered

GaAs/InAs self-assembled quantum dot structures for infrared detectors,” *J. Appl. Phys.* **104**, 113115 (2008).

A major challenge faced in the growth of heterostructures involving materials with high ( $>\sim 2\%$ ) lattice mismatch (needed to drive the formation of 3D islands that turn into quantum dots upon capping) is how to suppress the formation of extended defects that form to relieve the build-up of the strain with growing number of SAQD layers. One significant achievement of this program is the successful growth of extended defect-free multiple quantum dot (MQD) structures for up to 20-period, *while maintaining the uniformity and densities of SAQDs throughout the entire multiple layers*. To form such extended defect-free uniform MQD structures, we carried out MBE growth of 2.1 mono-layer (ML) shallow InAs SAQDs capped with 20 ML of  $\text{In}_{0.15}\text{Ga}_{0.85}\text{As}$  strain relieving layer followed by 130 ML GaAs spacer layers. The  $\text{In}_{0.15}\text{Ga}_{0.85}\text{As}$  strain relieving layer and the first 20 ML of GaAs spacer layers were grown at low-temperatures ( $350^\circ\text{C} - 400^\circ\text{C}$ ) exploiting migration enhanced epitaxy (MEE) in order to enhance adatom migration length even at such extremely low temperature needed to minimize the intermixing of InAs and GaAs. We note that the use of low temperature MEE for the growth of the island capping layers is a practice introduced by this PI’s group in 1993 at the initiation of the field of self-assembled quantum dots and has since been the unique signature of this group’s efforts in this field.

Extensive structural studies were carried out using cross-sectional transmission electron microscopy (XTEM) (Fig. 1.1) and, for the first time, large area plan-view TEM studies (Fig. 1.2) for such thick MQD structures. Employing appropriate imaging conditions ( $\mathbf{g} = \{220\}$  and  $\{400\}$ ), we unambiguously demonstrated that there are no observable extended defect formed in the above noted MQD structures up to 20 SAQD layers. Correspondingly, the sub-GaAs bandgap excitation photoluminescence (PL) spectra (Fig. 1.3) revealed no degradation in luminescence efficiency of SAQDs with the increasing number of SAQD layers. The peak positions and full width at half maximum (FWHM) of the PL spectra are also maintained up to 20-period thickness, indicating that a uniform SAQD distribution is maintained throughout the 20 layers. These systematic studies indicate that InAs islands on GaAs(001) and the combination of InGaAs/GaAs layers as capping/spacer layer, grown using protocols and conditions delineated here, accommodate effectively the accumulated strain to give uniform defect-free SAQD layers.

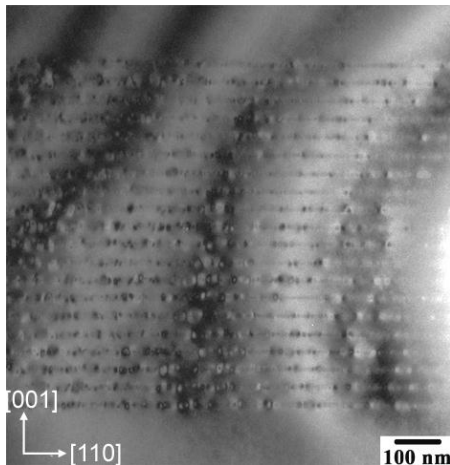


Fig. 1.1 Cross-sectional TEM image (bright field,  $\mathbf{g} = (220)$ ) of the 20-period MQD structure. No indication of extended defects or reduction of SAQD density in upper layers is observed.

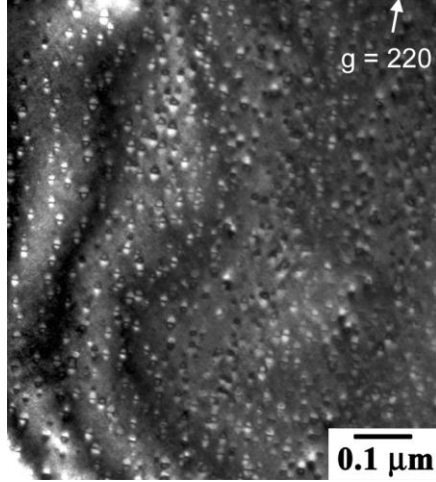


Fig. 1.2 Large area plan-view TEM image (dark field,  $g = (220)$ ) of the top 1 – 3 layers of the 20-period MQD structure. No dislocation is observed, and the SAQD density is maintained at  $\sim 4 \times 10^{10} / \text{cm}^2$  per SAQD layer, identical to the density at the bottom layer.

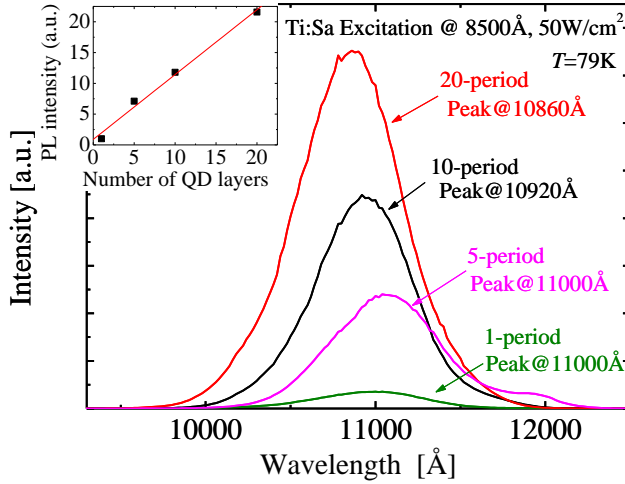


Fig. 1.3 PL spectra of MQD structures with various numbers of SAQD layers (1- to 20-period). The inset shows linear increase of total integrated intensity as a function of number of SAQD layers, indicating no degradation of SAQD emission efficiency with increasing SAQD layers. The peak position and width are almost constant for all the 1- to 20-period MQD structures.

## II. 2 Self-consistent charge distribution and electric potential profile in QDIP structures and its impact on QDIP characteristics

**Publication:** Tetsuya Asano, Anupam Madhukar, Krishnamurthy Mahalingam, and Gail J. Brown, “Dark current and band profiles in low defect density thick multilayered GaAs/InAs self-assembled quantum dot structures for infrared detectors,” *J. Appl. Phys.* **104**, 113115 (2008).

Having realized the high quality MQD structures discussed in the preceding section, we undertook a systematic study of QDIPs involving such MQDs designed and grown as the MIR or LWIR absorption regions sandwiched between n-doped GaAs regions to give n-i(MQD)-n QDIP structures.. The **second significant achievement** in this program thus relates to the semi-quantitative determination of the self-consistent electrical potential profile and electron density distribution in the QDIP structures which together determine the QDIP (opto)electronic characteristics (the dark and photocurrent behaviors). This study shed light on the unaddressed question concerning the dependence of the QDIP device characteristics on its structural parameters (such as the number of SAQD layers and the spacer thickness), and the doping profile etc.

Our temperature dependent dark current (DC) studies of  $n-i-n$  QDIP structures with 5- to 20-period showed that the DC activation energies increased with increasing number of SAQD layers and continuously decreased with increasing applied bias (Fig. 2.1). This indicates that the DC activation energy represents the built-in potential in the active region of the QDIP structures. Separately, ionization energy of the SAQDs was measured to be  $\sim 225$  meV using the PC spectrum. From these two measured values (built-in potential and the QD ionization energies), we obtained the SAQD energy levels with respect to Fermi energy, and hence, electron occupancy in SAQDs as shown in Fig. 2.2. This analysis revealed that, for the doping schemes employed, all the SAQDs in the 5-period  $n-i-n$  QDIP were occupied with electrons whereas most of the SAQDs in 20-period  $n-i-n$  QDIP did not have electrons in them. This study provided the guidance to the optimum doping profile for highest PC with lowest possible DC based on the self-consistent electron density profile and electric potential profile that depends on three-dimensional distribution of SAQD densities, doping profiles, and deep trap densities.

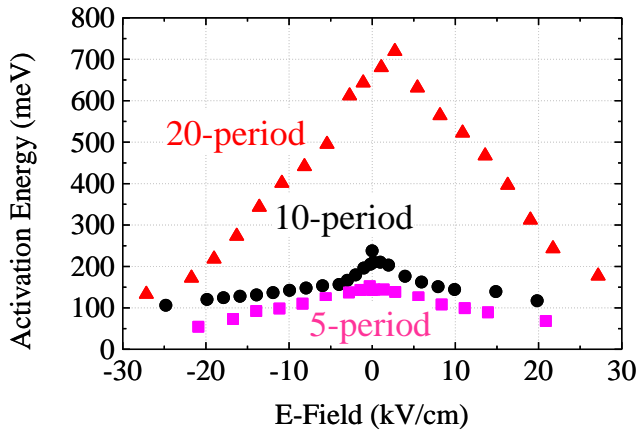


Fig. 2.1 DC activation energies of 5-period to 20-period of QDIP structures. The DC activation energy increases with increasing number of SAQD layers, and continuously decreases with increasing applied bias. This indicates that the DC activation energy represents the built-in potential of the active regions in the QDIP structures.

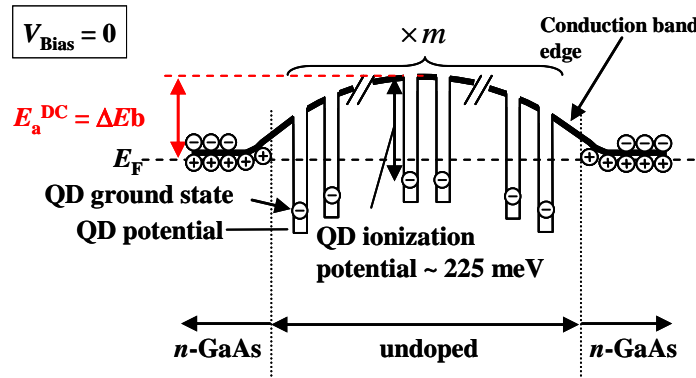


Fig. 2.2 Schematic conduction band edge profile of  $n-i-n$  QDIP structures with  $m$ -period. The DC activation energy ( $E_a^{DC}$ ) represents the built-in potential ( $\Delta E_b$ ) in the active region of the QDIP structure. From the relationship between  $E_a^{DC}$  and the QD ionization potential, the electron occupancy in the SAQDs can be semi-quantitatively estimated.

The high built-in potential of the QDIP structures (e.g., 720 meV for 20-period at zero applied bias (Fig. 2.1)) measured in our systematic characterization of QDIP

structures implied the presence of deep level traps in the QDIP structures at the density of  $\sim 10^{15} / \text{cm}^3$ . Such high density of deep level traps (*cf.* SAQD density is  $\sim 1 \times 10^{16} / \text{cm}^3$  with the typical SAQD sheet density [ $\sim 5 \times 10^{10} / \text{cm}^2$ ] and spacer thickness [ $\sim 50 \text{ nm}$ ]) may be the culprit for the limitations to QDIP performance because the deep level traps can drain electrons from QDs and/or can scatter the photo-excited carriers. Our recognition of the presence of deep levels in the QDIP structures led us to investigate the energies, densities, and spatial location of the deep traps and their influence on SAQD devices, as addressed in the next section.

### II.3 Study of deep levels in SAQD structures and their effect on electrical characteristics of SAQD devices

**Publication:** Tetsuya Asano, Zhaoqiang Fang, and Anupam Madhukar, “Deep levels in GaAs(001)/InAs/InGaAs/GaAs self-assembled quantum dot structures and their effect on quantum dot devices,” *J. Appl. Phys.* **107**, 073111 (2010).

The **third major accomplishment** under this program is the finding that the dominant deep level traps that adversely impact the electrical characteristics of the SAQD devices reside in the GaAs overgrowth layers (i.e. the GaAs spacer layers in the MQD structures), and their density depends critically of on the growth procedure and condition. Thus **a new growth approach and conditions for the GaAs spacer layers were identified that significantly reduce the deep level density and thus improve the QDIP electrical characteristics.**

To investigate the spatial density distribution and energy of the deep level traps present in SAQD structures, we performed deep level transient spectroscopy (DLTS) measurements on InAs/InGaAs/GaAs SAQD structures (Fig. 3.1) with different GaAs overlayer growth approaches (MBE vs MEE) and conditions. We found that different types of deep levels exist in different regions of the SAQD structures owing to different growth conditions (Fig. 3.2). The dominant deep level density ( $\sim 2 \times 10^{15} / \text{cm}^3$ ) was observed in the GaAs overgrowth layer grown by MBE at  $500^\circ \text{C}$ . This is the commonly employed growth condition for the GaAs overgrowth on InAs islands in the literature since at higher temperatures In evaporation as well as intermixing with the GaAs overlayer become significant and cause severe change in the characteristics of the island quantum dots. Our measurements showed that the binding energy of these deep levels present in the GaAs overgrowth layer is  $\sim 0.44 \text{ eV}$ , deeper than the SAQD ground state energy levels. Thus electrons from the dopants are trapped into these deep levels rather than being present in the SAQDs where they are needed for the absorption of the IR radiation and subsequent efficient transport.

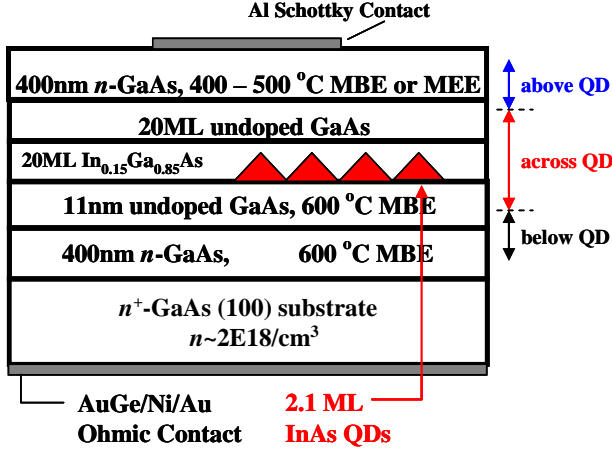


Fig. 3.1 Schematic of SAQD structures for DLTS measurements. The top overgrowth layer was grown either by 500 °C MBE, 500 °C MEE, or 400 °C MEE. The different regions investigated by DLTS are indicated by arrows on the right.

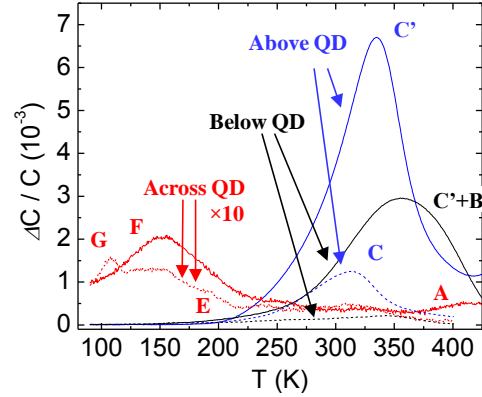


Fig. 3.2 DLTS spectra of an SAQD structure with overgrowth layer grown by 500 °C MBE. The dotted lines are the DLTS spectra of the control sample with no InAs or InGaAs layers were grown.

To reduce such high density of deep level traps in GaAs overgrowth layers, we replaced the MBE GaAs grown at 500°C by GaAs grown by MEE which can enhance the adatom migration length even at very low temperatures. Thus the GaAs spacer layers were grown by MEE at 400 °C or 500 °C. This significantly reduced the deep level density by a factor of ~ 20 (Fig. 3.3) compared to the 500°C MBE GaAs.

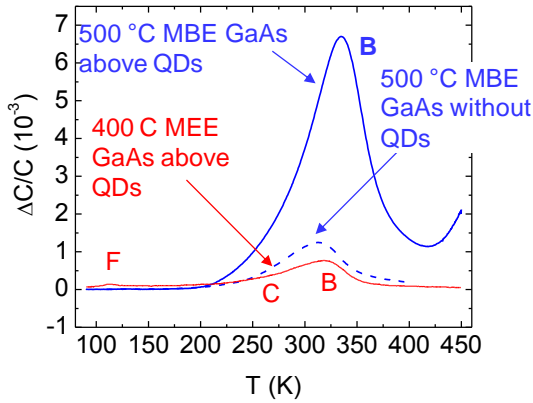
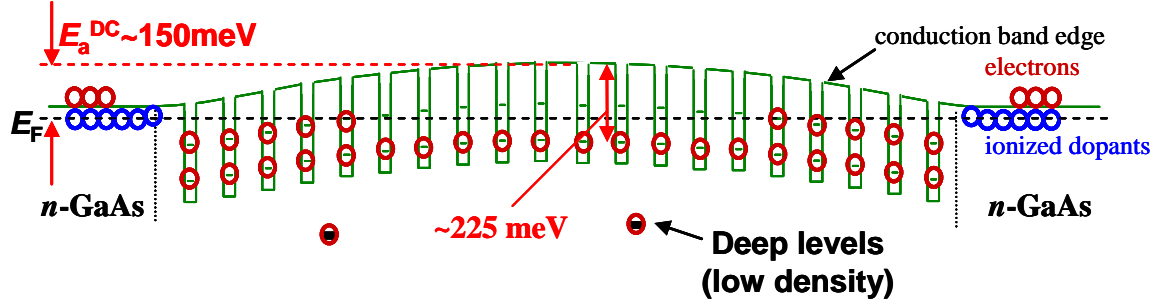


Fig. 3.3 DLTS spectra of overgrowth layers of SAQD structures with different growth conditions (500 °C MBE vs 400 °C MEE). Reduction of deep level density by factor of ~ 20 in the MEE-grown GaAs overlayer compared to the 500 °C MBE-grown overlayer was revealed.

Such a large deep level density variation with the choice of the growth approach and conditions is found to make a huge impact on the QDIP characteristics. We grew the  $n-i$  (20-period)  $-n$  QDIP structures with GaAs spacers grown by MEE at 500 °C and compared its DC activation energy with that of the identical 20-period QDIP structure but with the GaAs spacers grown by MBE at 500 °C. The built-in potential of the QDIP with 500 °C MEE GaAs spacers is ~ 150 meV (Fig. 3.4 (a)) as opposed to ~ 720 meV for the QDIP with the 500 °C MBE GaAs spacers (Fig. 3.4 (b)). This indicates that all the

SAQDs in the QDIP with 500 °C MEE GaAs spacers are filled with electrons at zero-applied bias, as opposed to the QDIP with 500 °C MBE GaAs spacers where most of the SAQD layers are depleted owing to the trapping of the electrons in the deep levels of the 500°C MBE GaAs. This study thus not only points to the significant impact of the deep levels present in GaAs overlayer on the SAQD device characteristics, but also reveals the importance of the appropriate growth procedure and conditions employed for GaAs overgrowth to reduce the deleterious deep level densities.

**(a) 500 °C MEE grown GaAs spacers**



**(b) 500 °C MBE-grown GaAs spacers**

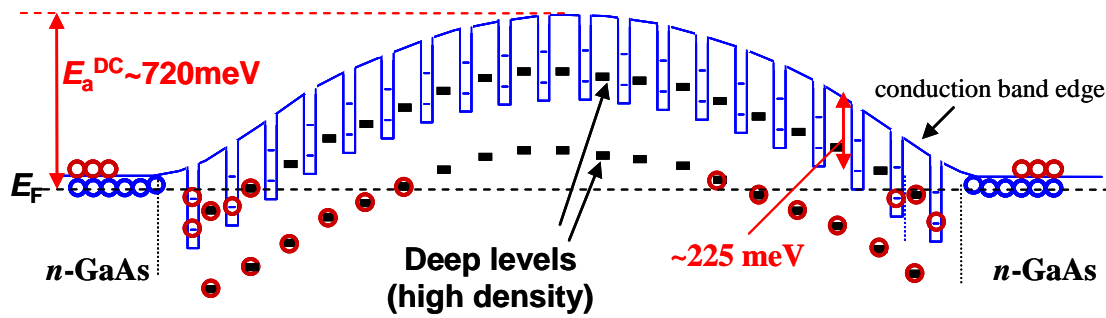


Fig. 3.4 Schematic conduction band edge profiles of 20-period QDIP structures (a) with the spacer layers grown by 500 °C MEE, and (b) by 500 °C MBE commonly employed in literature. With MEE GaAs spacers, all the SAQDs are occupied with electrons (a), as opposed to the MBE GaAs spacers where most of SAQDs are depleted with electrons (b). This clearly demonstrates the impact of deep level densities on QDIP device characteristics, and importance of the growth conditions of spacer layers.

## II. 4 Design and implementation of resonant cavity-enhanced QDIP

**Publication:** Tetsuya Asano, Chong Hu, Yi Zhang, Mingguo Liu, Joe C. Campbell, and Anupam Madhukar, “Design Consideration and Demonstration of Resonant Cavity-Enhanced Quantum Dot Infrared Photodetectors in Mid Infrared Wavelength Regime (3 – 5  $\mu\text{m}$ ),” *IEEE J. Quantum Electron.* (In Press).

The **fourth significant achievement** made in this program is the successful implementation of a resonant cavity QDIP structure for enhancement of the light intensity in the absorption region of the QDIP. Incorporating the QDIP structures

discussed in the preceding sections in a suitably designed resonant cavity, we demonstrated an enhancement of the QDIP detectivity by a factor of  $\sim 10$ .

To effectively enhance QDIP performance using a resonant cavity, it is of utmost importance to realize a narrow QD photoresponse peak width comparable to or narrower than the resonant cavity bandwidth. In this regard, we have recognized that bound-to-bound transitions in SAQDs exhibit narrow *intraband* photoresponse. In order to have a bound-to-bound intraband transition in InAs SAQDs in the MIR regime of interest, we confined the InAs SAQDs with GaAs and  $[(\text{AlAs})_1(\text{GaAs})_4]_4$  short period superlattices (SPSLs) rather than InGaAs/GaAs. The QDIP structure comprises 5 periods of  $\{[(\text{AlAs})_1(\text{GaAs})_4]_4 / 2 \text{ ML InAs SAQDs} / 12 \text{ ML GaAs} / [(\text{AlAs})_1(\text{GaAs})_4]_4 / 98 \text{ ML GaAs}\}$  MQD structure. The PC spectra of this MQD structure exhibited a peak at  $\sim 4.4 \mu\text{m}$  with FWHM  $\sim 0.4 \mu\text{m}$ , giving rise to  $\Delta\lambda / \lambda \sim 10 \%$  (Fig.4.1). This is the narrowest InAs/InAlGaAs SAQD photoresponse reported within the MIR regime.

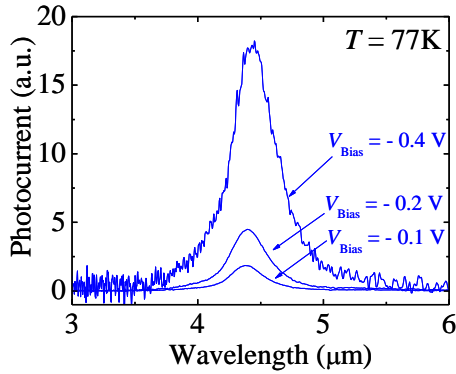


Fig. 4.1 Photocurrent spectra of the 5-period of InAs SAQDs sandwiched with  $[(\text{AlAs})_1(\text{GaAs})_4]_4$  SPSLs. Narrow MIR response ( $\Delta\lambda / \lambda \sim 10 \%$ ) is clearly observed, which is attributed to a bound-to-bound transition.

Having achieved extremely narrow MIR response QDIPs, we incorporated these in an appropriately designed resonant cavity to enhance absorption. The design of the resonant cavity is based on our modeling and simulations of the light intensity profile in a Fabry-Perot cavity. The bottom mirror was chosen to be a pair of GaAs/air-gap layers giving 98 % reflectance. Owing to the large refractive index discontinuity between GaAs and air ( $n_{\text{GaAs}} / n_{\text{air}} \sim 3.3 / 1$ ), such a high reflectance is realized with only a pair of these bilayers ( $\sim 3 \mu\text{m}$  thick), which significantly reduces the burden of otherwise unfeasibly thick ( $> \sim 10 \mu\text{m}$ ) growth required if the mirror were to be made from GaAs/AlGaAs layers (as routinely employed in near IR devices). For the top mirror, we employed the low reflectance from the GaAs surface ( $\sim 30 \%$  reflection). This broadens the resonant cavity peak width to  $\sim 0.2 \mu\text{m}$  thereby covering a much larger fraction of the SAQD MIR response peak than the high-Q resonant cavities typically used for monochromatic photodetectors. As shown in Fig.4.2, this resonant cavity provides  $\sim 12$  times enhancement of the peak light intensity. Note also the spatial locations (Fig.4.2, red bars) of the intensity enhancement, indicating these regions to be best suited for the placement of the SAQDS (rather than the continuous placement employed in all previous work).

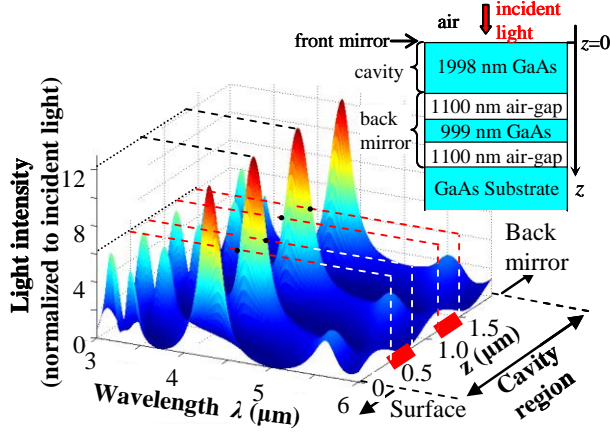


Fig. 4.2 Simulated light intensity profile in the resonant cavity structure as a function of the wavelength. The red bars on the  $z$ -axis indicates the region within the half-maximum of the intensity peaks, where MQD structures were to be grown. The inset shows the model structure on which simulation was performed.

The resonant cavity QDIP (RC-QDIP) structures were designed in coordination with the light intensity distribution inside the cavity as noted above. A 7-period SAQD structure was placed within the half-maximum spatial region of each of the two light intensity peaks. The valley region in between was then utilized to advantage by doping it to provide electrons to the 7-period SAQD structures on either side, as guided by the knowledge on doping established in Sec. II.2. The cavity length was tuned by etching the top GaAs layer to match the resonant wavelength to the QD photoresponse peak wavelength. After undercutting AlGaAs sacrificial layers to form air-gap/GaAs back mirror, we obtained the RC-QDIP. The measured detectivity as a function of applied bias at 80K for this RC-QDIP and its control device with identical QDIP but no resonant cavity is shown in Fig.4.3. An enhancement of a factor of  $\sim 12$  in the peak detectivity is realized using the resonant cavity. This is the first demonstration of resonant cavity enhancement for a MIR photodetector. The absolute value of the resonant cavity enhanced detectivity is about an order of magnitude lower than the best values reported in the literature by several groups including [refs]. This, however, is a consequence of the particular prevailing background impurity conditions of the growth chamber at the time of the growth of these samples as is manifest in the two orders of magnitude lower detectivity of the control QDIP (i.e. without the resonant cavity). The observed enhancement by a factor of  $\sim 10$ , as the design and simulations predicted, shows that when the state-of-the-art non-resonant cavity QDIPs with detectivities  $\sim E10$  to  $E11$  are placed in the resonant cavity, QDIPs with detectivities greater than  $E11$  can now be consistently realized.

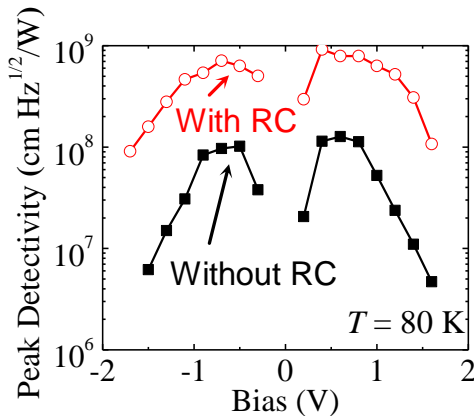


Fig. 4.3 Detectivity of a MIR-QDIP with and without the resonant cavity. An enhancement in the detectivity by factor of  $\sim 10$  is demonstrated. RC stands for resonant cavity.

### **III. Personnel Supported**

#### **Graduate Students:**

T. Asano (PhD, USC); S. Lu (PhD, USC); Y. Zhang (MS, USC); Z. Lingley (PhD, USC); M. Liu (PhD, UVa); C. Hu (PhD, UVa)

#### **Postdocs**

S. Lu (USC)

### **IV. Publications**

1. Tetsuya Asano, Anupam Madhukar, Krishnamurthy Mahalingam, and Gail J. Brown, "Dark current and band profiles in low defect density thick multilayered GaAs/InAs self-assembled quantum dot structures for infrared detectors," *J. Appl. Phys.* **104**, 113115 (2008).
2. Tetsuya Asano, Zhaoqiang Fang, and Anupam Madhukar, "Deep levels in GaAs(001)/InAs/InGaAs/GaAs self-assembled quantum dot structures and their effect on quantum dot devices," *J. Appl. Phys.* **107**, 073111 (2010).
3. Tetsuya Asano, Chong Hu, Yi Zhang, Mingguo Liu, Joe C. Campbell, and Anupam Madhukar, "Design Consideration and Demonstration of Resonant Cavity-Enhanced Quantum Dot Infrared Photodetectors in Mid Infrared Wavelength Regime (3 – 5  $\mu\text{m}$ )," *IEEE J. Quantum Electron.* (In Press).

### **V. Conference presentations**

1. Tetsuya Asano, Krishnamurthy Mahalingam, and Anupam Madhukar, "Study of Structural, Optical, and Photocurrent Behavior of Thick Multilayered Self-Assembled Quantum Dot InAs/InGaAs Structures as a Function of Doping," The 34th International Symposium on Compound Semiconductors, Kyoto, Japan, Oct. 15-18, 2007.
2. Tetsuya Asano, Krishnamurthy Mahalingam, Zhaoqiang Fang, and Anupam Madhukar, "Systematic Study of Structure and Current Transport in Low Defect Density Thick Multilayered GaAs/InAs Self-Assembled Quantum Dot Structures for Infrared Detectors," 50th TMS Electronic Materials Conference, Santa Barbara, CA, June 25-27, 2008.
3. Tetsuya Asano, Zhaoqiang Fang, and Anupam Madhukar, "Deep Level Traps in Single and Multiple InAs/(InGaAs)/GaAs Self-Assembled Quantum Dot Structures," 51st TMS Electronic Materials Conference, University Park, PA, June 24-26, 2009.